10

Determination of Crystal Structure

10–1 INTRODUCTION

Since 1913, when W. L. Bragg solved the structure of NaCl, the structures of many thousands of crystals, organic and inorganic, have been determined. This vast body of knowledge is of fundamental importance in such fields as crystal chemistry, solid-state physics, and the biological sciences because, to a large extent, structure determines properties and the properties of a substance are never fully understood until its structure is known. In metallurgy, a knowledge of crystal structure is a necessary prerequisite to any understanding of such phenomena as plastic deformation, alloy formation, or phase transformations.

The work of structure determination goes on continuously since there is no dearth of unsolved structures. New substances are constantly being synthesized, and the structures of many old ones are still unknown. In themselves crystal structures vary widely in complexity: the simplest can be solved in a few hours, while the more complex may require months or even years for their complete solution. (Proteins form a notable example of the latter kind; some protein structures are now known, but others still defy solution.) Complex structures require complex methods of solution, and structure determination in its entirety is more properly the subject of a book than of a single chapter. All we can do here is to consider some of the principles involved and how they can be applied to the solution of fairly simple structures. Moreover, we will confine our attention to the methods of determining structure from powder patterns alone, because such patterns are the kind most often encountered by the metallurgist.

The basic principles involved in structure determination have already been introduced in Chaps. 3 and 4. We saw there that the crystal structure of a substance determines the diffraction pattern of that substance or, more specifically, that the shape and size of the unit cell determines the angular positions of the diffraction lines, and the arrangement of the atoms within the unit cell determines the relative intensities of the lines. It may be worthwhile to state this again in tabular form:

Crystal structure		Diffraction pattern
Unit cell	↔	Line positions
Atom positions	↔	Line intensities

Since structure determines the diffraction pattern, it should be possible to go in the

other direction and deduce the structure from the pattern. It is possible, *but not in any direct manner*. Given a structure, we can calculate its diffraction pattern in a very straightforward fashion, and examples of such calculations were given in Sec. 4–13; but the reverse problem, that of directly calculating the structure from the observed pattern, has not yet been solved for the general case (Sec. 10–8). The procedure adopted is essentially one of trial and error. On the basis of an educated guess, a structure is assumed, its diffraction pattern calculated, and the calculated pattern compared with the observed one. If the two agree in all detail, the assumed structure is correct; if not, the process is repeated as often as is necessary to find the correct solution. The problem is not unlike that of deciphering a code, and requires of the crystallographer the same qualities possessed by a good cryptanalyst, namely, knowledge, perseverance, and not a little intuition.

The determination of an unknown structure proceeds in three major steps:

1. The shape and size of the unit cell are deduced from the angular positions of the diffraction lines. An assumption is first made as to which of the seven crystal systems the unknown structure belongs to, and then, on the basis of this assumption, the correct Miller indices are assigned to each reflection. This step is called "indexing the pattern" and is possible only when the correct choice of crystal system has been made. Once this is done, the shape of the unit cell is known (from the crystal system), and its size is calculable from the positions and Miller indices of the diffraction lines.

2. The number of atoms per unit cell is then computed from the shape and size of the unit cell, the chemical composition of the specimen, and its measured density.

3. Finally, the positions of the atoms within the unit cell are deduced from the relative intensities of the diffraction lines.

Only when these three steps have been accomplished is the structure determination complete. The third step is generally the most difficult, and there are many structures which are known only incompletely, in the sense that this final step has not yet been made. Nevertheless, a knowledge of the shape and size of the unit cell, without any knowledge of atom positions, is in itself of very great value in many applications.

The average metallurgist is rarely, if ever, called upon to determine an unknown crystal structure. If the structure is at all complex, its determination is a job for a specialist in x-ray crystallography, who can bring special techniques, both experimental and mathematical, to bear on the problem. The metallurgist should, however, know enough about structure determination to unravel any simple structures he may encounter and, what is more important, he must be able to index the powder patterns of substances of *known* structure, as this is a routine problem in almost all diffraction work. The procedures given below for indexing patterns are applicable whether the structure is known or not, but they are of course very much easier to apply if the structure is known beforehand.

10–2 PRELIMINARY TREATMENT OF DATA

The powder pattern of the unknown is obtained with a Debye–Scherrer camera or a diffractometer, the object being to cover as wide an angular range of 2θ as possible. A camera such as the Seemann–Bohlin, which records diffraction lines over only a limited angular range, is of very little use in structure analysis. The specimen preparation must ensure random orientation of the individual particles of powder, if the observed relative intensities of the diffraction lines are to have any meaning in terms of crystal structure. After the pattern is obtained, the value of $\sin^2 \theta$ is calculated for each diffraction line; this set of $\sin^2 \theta$ values is the raw material for the determination of cell size and shape. Or one can calculate the d value of each line and work from this set of numbers.

Since the problem of structure determination is one of finding a structure which will account for all the lines on the pattern, in both position and intensity, the investigator must make sure at the outset that the observed pattern does not contain any extraneous lines. The ideal pattern contains lines formed by x-rays of a single wavelength, diffracted only by the substance whose structure is to be determined. There are therefore two sources of extraneous lines:

1. *Diffraction of x-rays having wavelengths different from that of the principal component of the radiation.* If filtered radiation is used, then $K\alpha$ radiation is the principal component, and characteristic x-rays of any other wavelength may produce extraneous lines. The chief offender is $K\beta$ radiation, which is never entirely removed by a filter and may be a source of extraneous lines when diffracted by lattice planes of high reflecting power. The presence of $K\beta$ lines on a pattern can usually be revealed by calculation, since if a certain set of planes reflect $K\beta$ radiation at an angle θ_β, they must also reflect K_α radiation at an angle θ_α (unless θ_α exceeds 90°), and one angle may be calculated from the other. It follows from the Bragg law that

$$\left(\frac{\lambda^2_{K\alpha}}{\lambda^2_{K\beta}}\right) \sin^2 \theta_\beta = \sin^2 \theta_\alpha, \tag{10–1}$$

where $\lambda^2_{K\alpha}/\lambda^2_{K\beta}$ has a value near 1.2 for most radiations. If it is suspected that a particular line is due to $K\beta$ radiation, multiplication of its $\sin^2 \theta$ value by $\lambda^2_{K\alpha}/\lambda^2_{K\beta}$ will give a value equal, or nearly equal, to the value of $\sin^2 \theta$ for some $K\alpha$ line on the pattern, unless the product exceeds unity. The $K\beta$ line corresponding to a given $K\alpha$ line is always located at a smaller angle 2θ and has lower intensity. However, since $K\alpha$ and $K\beta$ lines (from different planes) may overlap on the pattern, Eq. (10–1) alone can establish only the possibility that a given line is due to $K\beta$ radiation, but it can never prove that it is. Another possible source of extraneous lines is L characteristic radiation from tungsten contamination on the target of the x-ray tube, particularly if the tube is old. If such contamination is suspected, equations such as (10–1) can be set up to test the possibility that certain lines are due to tungsten radiation.

2. *Diffraction by substances other than the unknown.* Such substances are usually impurities in the specimen but may also include the specimen mount or badly

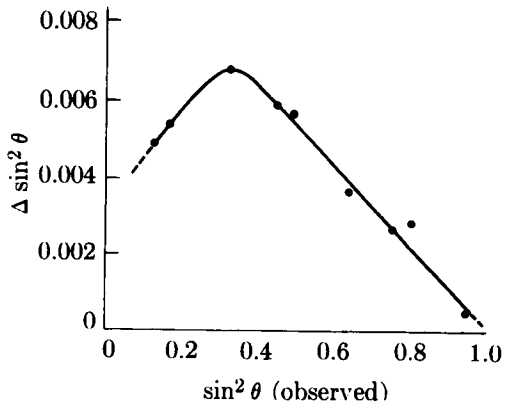

Fig. 10–1 An example of a correction curve for $\sin^2 \theta$ values.

aligned slits. Careful specimen preparation and good experimental technique will eliminate extraneous lines due to these causes.

For reasons to be discussed in Chap. 11, the observed values of $\sin^2 \theta$ always contain small systematic errors. These errors are not large enough to cause any difficulty in indexing patterns of cubic crystals, but they can seriously interfere with the determination of some noncubic structures. The best method of removing such errors from the data is to calibrate the camera or diffractometer with a substance of known lattice parameter, mixed with the unknown. The difference between the observed and calculated values of $\sin^2 \theta$ for the standard substance gives the error in $\sin^2 \theta$, and this error can be plotted as a function of the observed values of $\sin^2 \theta$. Figure 10–1 shows a correction curve of this kind, obtained with a particular specimen and a particular Debye-Scherrer camera.* The errors represented by the ordinates of such a curve can then be applied to each of the observed values of $\sin^2 \theta$ for the diffraction lines of the unknown substance. For the particular determination represented by Fig. 10–1, the errors shown are to be subtracted from the observed values.

10–3 INDEXING PATTERNS OF CUBIC CRYSTALS

A cubic crystal gives diffraction lines whose $\sin^2 \theta$ values satisfy the following equation, obtained by combining the Bragg law with the plane-spacing equation for the cubic system, as in Eq. (3–10):

$$\frac{\sin^2 \theta}{(h^2 + k^2 + l^2)} = \frac{\sin^2 \theta}{s} = \frac{\lambda^2}{4a^2}. \tag{10–2}$$

Since the sum $s = (h^2 + k^2 + l^2)$ is always integral and $\lambda^2/4a^2$ is a constant for any one pattern, the problem of indexing the pattern of a cubic substance is one of finding a set of integers s which will yield a constant quotient when divided one by one into the observed $\sin^2 \theta$ values. (Certain integers, such as 7, 15, 23, 28, 31,

* For the shape of this curve, see Prob. 11–5.

etc., are impossible because they cannot be formed by the sum of three squared integers.) Once the proper integers s are found, the indices hkl of each line can be written down by inspection or from the tabulation in Appendix 10.

The proper set of integers s is not hard to find because there are only a few possible sets. Each of the four common cubic lattice types has a characteristic sequence of diffraction lines, described by their sequential s values:

Simple cubic: 1, 2, 3, 4, 5, 6, 8, 9, 10, 11, 12, 13, 14, 16, . . .
Body-centered cubic: 2, 4, 6, 8, 10, 12, 14, 16, . . .
Face-centered cubic: 3, 4, 8, 11, 12, 16, . . .
Diamond cubic: 3, 8, 11, 16, . . .

Each set can be tried in turn. Longer lists can be prepared from Appendix 10. If a set of integers satisfying Eq. (10–2) cannot be found, then the substance involved does not belong to the cubic system, and other possibilities (tetragonal, hexagonal, etc.) must be explored.

The following example will illustrate the steps involved in indexing the pattern of a cubic substance and finding its lattice parameter. In this particular example, Cu $K\alpha$ radiation was used and eight diffraction lines were observed. Their $\sin^2\theta$ values are listed in the second column of Table 10–1. After a few trials, the integers s listed in the third column were found to produce the reasonably constant quotients listed in the fourth column, when divided into the observed $\sin^2\theta$ values. The fifth column lists the lattice parameter calculated from each line position, and the sixth column gives the Miller indices of each line. The systematic error in $\sin^2\theta$ shows up as a gradual decrease in the value of $\lambda^2/4a^2$, and a gradual increase in the value of a, as θ increases. We shall find in Chap. 11 that the systematic error in a decreases as θ increases; therefore we can select the value of a for the highest-angle line, namely, 3.62 Å, as being the most accurate of those listed. Our analysis of line positions therefore leads to the conclusion that the substance involved, copper in this case, is cubic in structure with a lattice parameter of 3.62 Å.

We can also determine the Bravais lattice of the specimen by observing which lines are present and which absent. Examination of the sixth column of Table 10–1

Table 10–1

1	2	3	4	5	6
Line	$\sin^2\theta$	$s = (h^2 + k^2 + l^2)$	$\frac{\lambda^2}{4a^2}$	a(Å)	hkl
1	0.140	3	0.0467	3.57	111
2	0.185	4	0.0463	3.59	200
3	0.369	8	0.0461	3.59	220
4	0.503	11	0.0457	3.61	311
5	0.548	12	0.0457	3.61	222
6	0.726	16	0.0454	3.62	400
7	0.861	19	0.0453	3.62	331
8	0.905	20	0.0453	3.62	420

shows that all lines which have mixed odd and even indices, such as 100, 110, etc., are absent from the pattern. Reference to the rules relating Bravais lattices to observed and absent reflections, given in Table 4–1, shows that the Bravais lattice of this specimen is face-centered. We now have certain information about the arrangement of atoms within the unit cell, and it should be noted that we have had to make use of observed line intensities in order to obtain this information. In this particular case, the observation consisted simply in noting which lines had zero intensity.

The characteristic line sequences for cubic lattices are shown graphically in Fig. 10–2, in the form of calculated diffraction patterns. The calculations are made for Cu $K\alpha$ radiation and a lattice parameter a of 3.50 Å. The positions of all the diffraction lines which would be formed under these conditions are indicated as they would appear on a film or chart of the length shown. (For comparative purposes, the pattern of a hexagonal close-packed structure is also illustrated, since this structure is frequently encountered among metals and alloys. The line positions are calculated for Cu $K\alpha$ radiation, $a = 2.50$ Å, and $c/a = 1.633$, which corresponds to the close packing of spheres.)

Powder patterns of cubic substances can usually be distinguished at a glance from those of noncubic substances, since the latter patterns normally contain many more lines. In addition, the Bravais lattice can usually be identified by inspection: there is an almost regular sequence of lines in simple cubic and body-centered cubic patterns, but the former contains almost twice as many lines, while a face-centered cubic pattern is characterized by a pair of lines, followed by a single line, followed by a pair, another single line, etc.

The problem of indexing a cubic pattern is of course very much simplified if the substance involved is *known* to be cubic and if the lattice parameter is also known. The simplest procedure then is to calculate the value of $\lambda^2/4a^2$ and divide this value into the observed $\sin^2\theta$ values to obtain the value of s for each line.

There is one difficulty that may arise in the interpretation of cubic powder patterns, and that is due to a possible ambiguity between simple cubic and body-centered cubic patterns. There is a regular sequence of lines in both patterns up to the sixth line; the sequence then continues regularly in body-centered cubic patterns, but is interrupted in simple cubic patterns since $s = 7$ is impossible. Therefore, if λ is so large, or a so small, that six lines or less appear on the pattern, the two Bravais lattices are indistinguishable. For example, suppose that the substance involved is actually body-centered cubic but the investigator mistakenly indexes it as simple cubic, assigning the value $s = 1$ to the first line, $s = 2$ to the second line, etc. He thus obtains a value of $\lambda^2/4a^2$ twice as large as the true one, and a value of a which is $1/\sqrt{2}$ times the true one. This mistake becomes apparent when the number of atoms per unit cell is calculated from the measured density of the specimen (Sec. 10–7); the wrong cell size will give a nonintegral value for the number of atoms per cell, and such a value is impossible. The ambiguity in the diffraction pattern itself can be avoided by choosing a wavelength short enough to produce at least seven lines on the pattern.

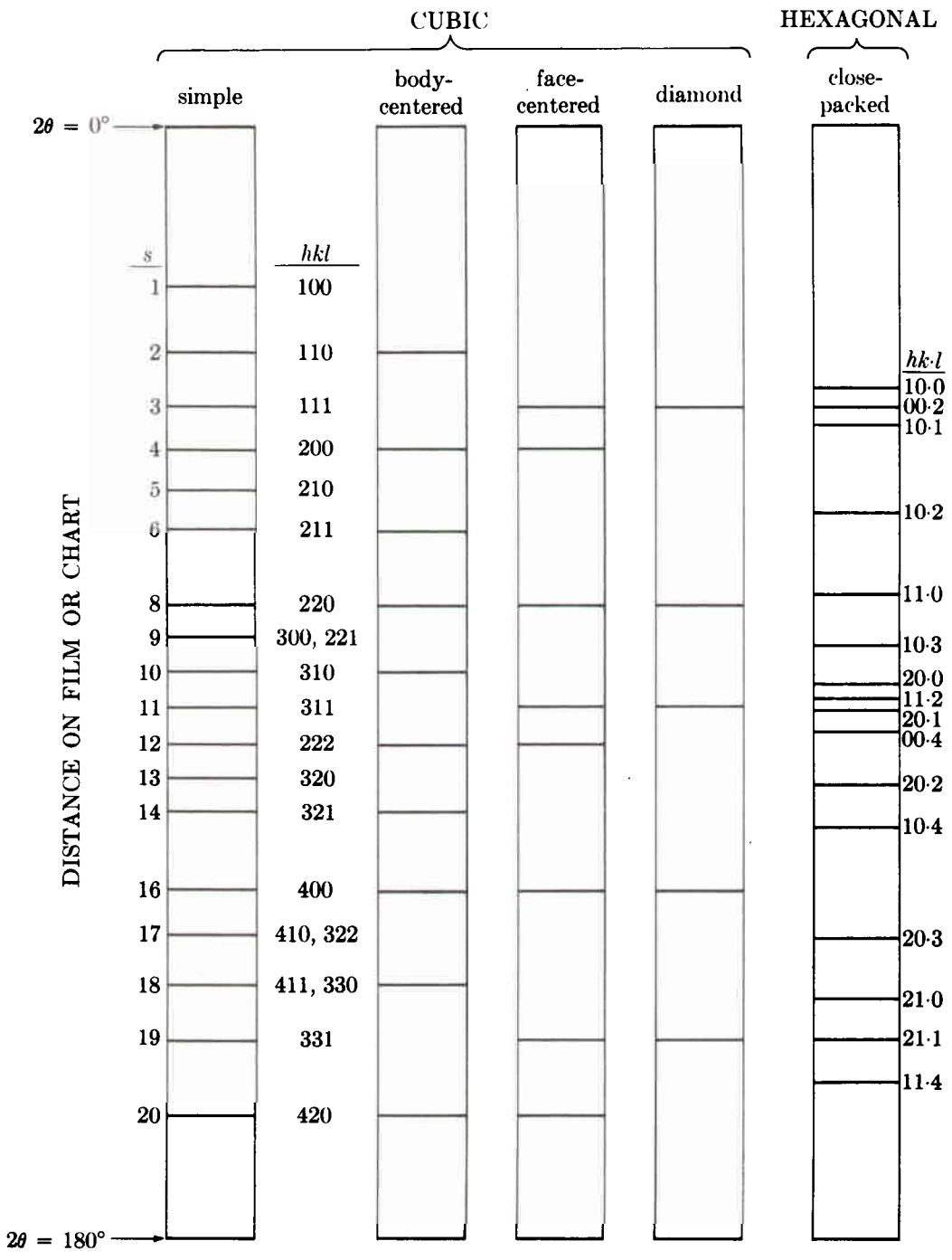

Fig. 10–2 Calculated diffraction patterns for various lattices. $s = h^2 + k^2 + l^2$.

10–4 INDEXING PATTERNS OF NONCUBIC CRYSTALS (GRAPHICAL METHODS)

The problem of indexing powder patterns becomes more difficult as the number of unknown parameters increases. There is only one unknown parameter for cubic crystals, the cell edge a, but noncubic crystals have two or more, and special graphical and analytical techniques have had to be devised in order to index the patterns of such crystals.

Tetragonal System

The plane-spacing equation for this system involves two unknown parameters, a and c:

$$\frac{1}{d^2} = \frac{h^2 + k^2}{a^2} + \frac{l^2}{c^2}. \tag{10–3}$$

This may be rewritten in the form

$$\frac{1}{d^2} = \frac{1}{a^2}\left[(h^2 + k^2) + \frac{l^2}{(c/a)^2}\right],$$

or

$$2 \log d = 2 \log a - \log\left[(h^2 + k^2) + \frac{l^2}{(c/a)^2}\right]. \tag{10–4}$$

Suppose we now write Eq. (10–4) for any two planes of a tetragonal crystal, distinguishing the two planes by subscripts 1 and 2, and then subtract the two equations. We obtain

$$2 \log d_1 - 2 \log d_2 = -\log\left[(h_1^2 + k_1^2) + \frac{l_1^2}{(c/a)^2}\right] + \log\left[(h_2^2 + k_2^2) + \frac{l_2^2}{(c/a)^2}\right]. \tag{10–5}$$

This equation shows that the difference between the 2 log d values for any two planes is independent of a and depends only on the axial ratio c/a and the indices hkl of each plane. This fact was used by Hull and Davey as the basis for a graphical method of indexing the powder patterns of tetragonal crystals [10.1].

The construction of a Hull–Davey chart is illustrated in Fig. 10–3. First, the variation of the quantity $[(h^2 + k^2) + l^2/(c/a)^2]$ with c/a is plotted on two-range semilog paper for particular values of hkl. Each set of indices hkl, as long as they correspond to planes of different spacing, produces a different curve, and when $l = 0$ the curve is a straight line parallel to the c/a axis. Planes of different indices but the same spacing, such as (100) and (010), are represented by the same curve on the chart, which is then marked with the indices of either one of them, in this case (100). [The chart shown is for a simple tetragonal lattice; one for a body-centered tetragonal lattice is made simply by omitting all curves for which $(h + k + l)$ is an odd number.] A single-range logarithmic d scale is then constructed; it extends over two ranges of the $[(h^2 + k^2) + l^2/(c/a)^2]$ scale and runs in the opposite direction, since the coefficient of log d in Eq. (10–4) is -2 times the coefficient of log $[(h^2 + k^2) + l^2/(c/a)^2]$. This means that the d values of two planes, for a given c/a ratio, are separated by the same distance on the scale as the horizontal separation, at the same c/a ratio, of the two corresponding curves on the chart.

The chart and scale are used for indexing in the following manner. The spacing d of the reflecting planes corresponding to each line on the diffraction pattern is calculated. Suppose that the first seven of these values for a particular pattern are 6.00, 4.00, 3.33, 3.00, 2.83, 2.55, and 2.40 Å. A strip of paper is first laid alongside

the d scale in position I of Fig. 10–3, and the observed d values are marked off on its edge with a pencil. The paper strip is then placed on the chart and moved about, both vertically and horizontally, until a position is found where each mark on the strip coincides with a line on the chart. Vertical and horizontal movements correspond to trying various c/a and a values, respectively, and the only restriction on these movements is that the edge of the strip must always be horizontal. When a correct fit has been obtained, as shown by position II of Fig. 10–3, the indices of each line are simply read from the corresponding curves, and the approximate value of c/a from the vertical position of the paper strip. In the present example, the c/a ratio is 1.5 and the first line on the pattern (formed by planes of spacing 6.00 Å) is a 001 line, the second a 100 line, the third a 101 line, etc. After all the lines have been indexed in this way, the d values of the two highest-angle lines are used to set up two equations of the form of Eq. (10–3), and these are solved simultaneously to yield the values of a and c. From these values, the axial ratio c/a may then be calculated with more precision than it can be found graphically.

Figure 10–3 is only a partial Hull–Davey chart. A complete one, showing curves of higher indices, is reproduced on a small scale in Fig. 10–4, which applies to body-centered tetragonal lattices. Note that the curves of high indices are often so crowded that it is difficult to assign the proper indices to the observed lines. It may then be necessary to calculate the indices of these high-angle lines on the basis of a and c values derived from the already indexed low-angle lines.

Some Hull–Davey charts, like the one shown in Fig. 10–4, are designed for use with $\sin^2\theta$ values rather than d values. No change in the chart itself is involved, only a change in the accompanying scale. This is possible because an equation similar to Eq. (10–4) can be set up in terms of $\sin^2\theta$ rather than d, by combining Eq. (10–3) with the Bragg law. This equation is

$$\log \sin^2\theta = \log \frac{\lambda^2}{4a^2} + \log\left[(h^2 + k^2) + \frac{l^2}{(c/a)^2}\right]. \qquad (10\text{–}6)$$

The $\sin^2\theta$ scale is therefore a two-range logarithmic one (from 0.01 to 1.0), equal in length to the two-range $[(h^2 + k^2) + l^2/(c/a)^2]$ scale on the chart and running in the same direction. A scale of this kind appears at the top of Fig. 10–3.

When the c/a ratio becomes equal to unity, a tetragonal cell becomes cubic. It follows that a cubic pattern can be indexed on a tetragonal Hull–Davey chart by keeping the paper strip always on the horizontal line corresponding to $c/a = 1$. (In fact, one can make one-dimensional Hull–Davey charts for the rapid indexing of cubic patterns.) It is instructive to consider a tetragonal cell as a departure from a cubic one and to examine a Hull–Davey chart in that light, since the chart shows at a glance how the powder pattern changes for any given change in the c/a ratio. It shows, for example, how certain lines split into two as soon as the c/a ratio departs from unity, and how even the order of the lines on the pattern can change with changes in c/a.

Another graphical method of indexing tetragonal patterns has been devised by Bunn [10.2]. Like the Hull–Davey chart, a Bunn chart consists of a network of curves, one for each value of *hkl*, but the curves are based on somewhat different functions of *hkl* and c/a than those used by Hull and Davey, with the result that

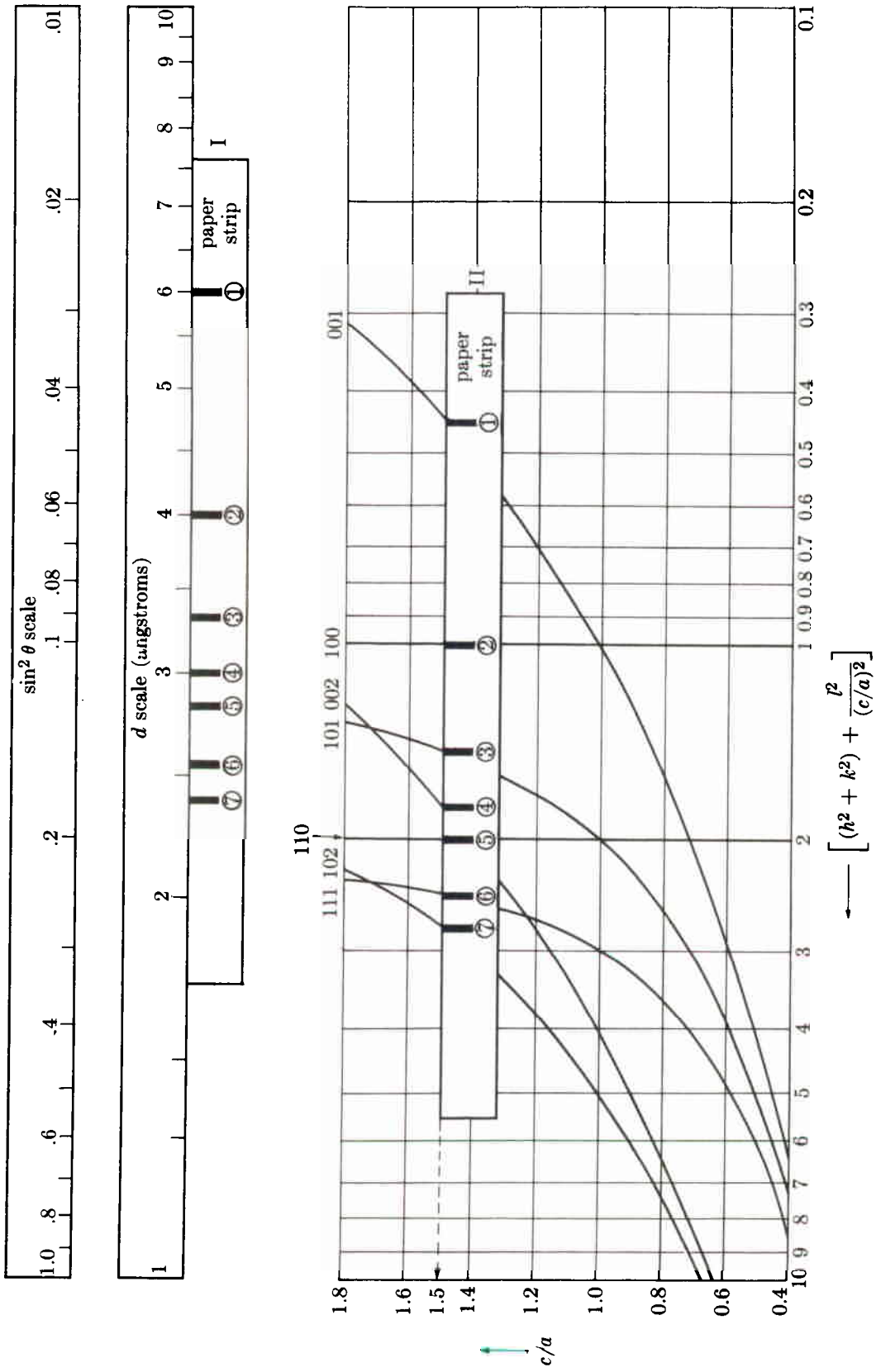

Fig. 10–3 Partial Hull–Davey chart for simple tetragonal lattices.

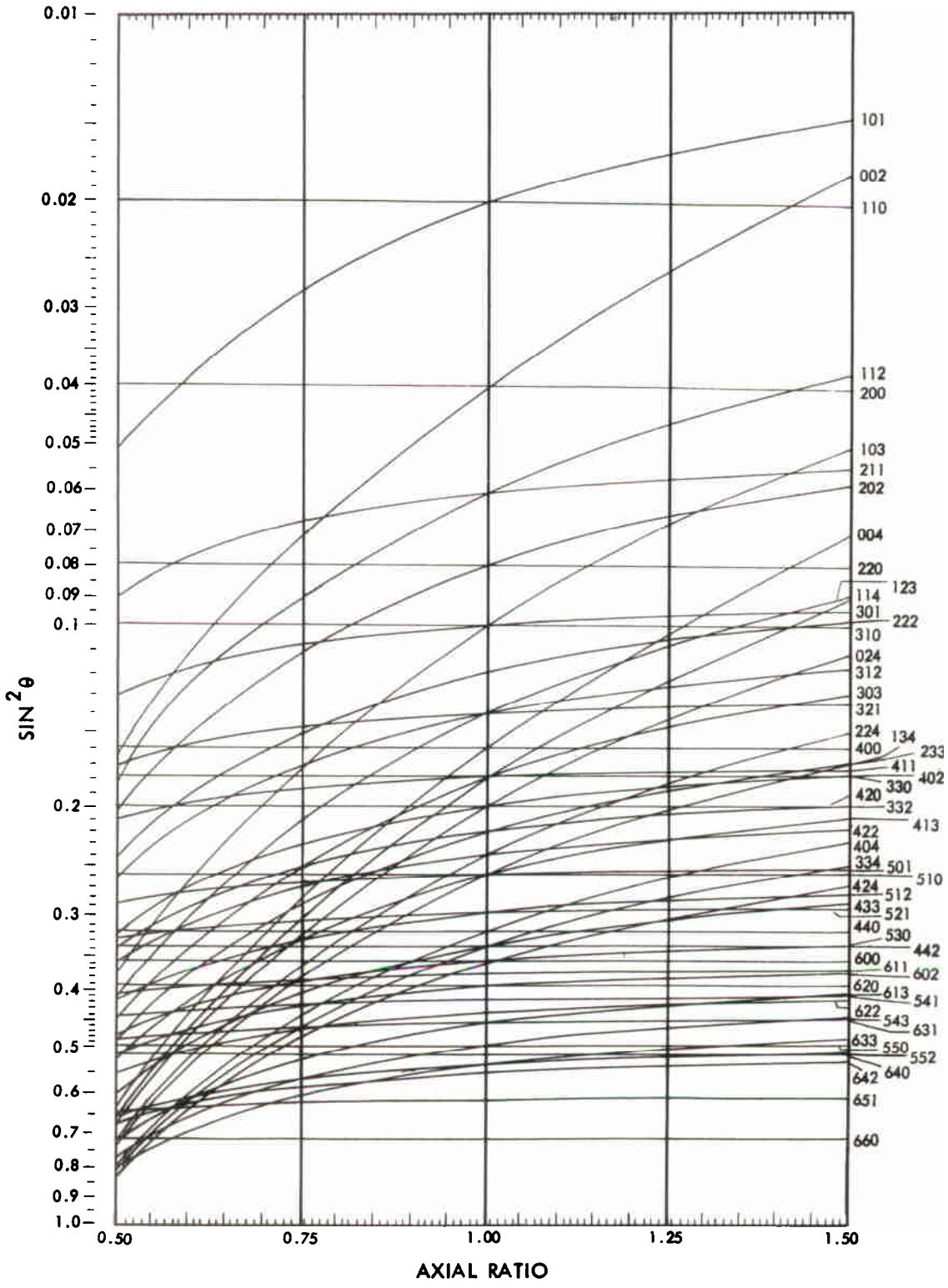

Fig. 10–4 Complete Hull–Davey chart for body-centered tetragonal lattices.

the curves are less crowded in certain regions of the chart. The Bunn chart is accompanied by a logarithmic scale of d values, and the combination of chart and scale is used in exactly the same way as a Hull–Davey chart and scale. Bunn charts may be purchased [10.3] or constructed from numerical data in [G.11, vol. 2, p. 207].

Hexagonal System

Patterns of hexagonal crystals can also be indexed by graphical methods, since the hexagonal unit cell, like the tetragonal, is characterized by two variable parameters, a and c. The plane-spacing equation is

$$\frac{1}{d^2} = \frac{4}{3} \cdot \frac{h^2 + hk + k^2}{a^2} + \frac{l^2}{c^2}.$$

After some manipulation, this becomes

$$2 \log d = 2 \log a - \log \left[\frac{4}{3} (h^2 + hk + k^2) + \frac{l^2}{(c/a)^2} \right],$$

which is of exactly the same form as Eq. (10–4) for the tetragonal system. A Hull–Davey chart for the hexagonal system can therefore be constructed by plotting the variation of $\log \left[\frac{4}{3}(h^2 + hk + k^2) + l^2/(c/a)^2 \right]$ with c/a. A Bunn chart may also be constructed for this system. Special charts for hexagonal close-packed lattices may also be prepared by omitting all curves for which $(h + 2k)$ is an integral multiple of 3 and l is odd.

The powder pattern of zinc made with Cu $K\alpha$ radiation (Fig. 3–13) will serve to illustrate how the pattern of a hexagonal substance is indexed. Thirteen lines were observed on this pattern; their $\sin^2 \theta$ values and relative intensities are listed in Table 10–2. A fit was obtained on a Hull–Davey chart for hexagonal close-packed lattices at an approximate c/a ratio of 1.87. The chart lines disclosed the indices listed in the fourth column of the table. In the case of line 5, two chart lines ($10 \cdot 3$ and $11 \cdot 0$) almost intersect at $c/a = 1.87$, so the observed line is evidently the sum of two lines, almost overlapping, one from the $(10 \cdot 3)$ planes and the other from $(11 \cdot 0)$ planes. The same is true of line 11. Four lines on the chart, namely, $20 \cdot 0$, $10 \cdot 4$, $21 \cdot 0$, and $20 \cdot 4$, do not appear on the pattern, and it must be inferred that these are too weak to be observed. On the other hand, all the observed lines are accounted for, so we may conclude that the lattice of zinc is actually hexagonal close-packed. The next step is to calculate the lattice parameters. Combination of the Bragg law and the plane-spacing equation gives

$$\sin^2 \theta = \frac{\lambda^2}{4} \left[\frac{4}{3} \cdot \frac{(h^2 + hk + k^2)}{a^2} + \frac{l^2}{c^2} \right],$$

where $\lambda^2/4$ has a value of 0.594 Å^2 for Cu $K\alpha$ radiation. Writing this equation out for the two highest-angle lines, namely, 12 and 13, we obtain:

$$0.806 = 0.594 \left(\frac{4}{3} \cdot \frac{7}{a^2} + \frac{1}{c^2} \right).$$

$$0.879 = 0.594 \left(\frac{4}{3} \cdot \frac{7}{a^2} + \frac{4}{c^2} \right).$$

Table 10–2

Line	Intensity	$\sin^2\theta$	*hk·l*
1	s	0.097	00·2
2	s	0.112	10·0
3	vs	0.136	10·1
4	m	0.209	10·2
5	s	0.332	10·3, 11·0
6	vw	0.390	00·4
7	m	0.434	11·2
8	m	0.472	20·1
9	vw	0.547	20·2
10	w	0.668	20·3
11	m	0.722	11·4, 10·5
12	m	0.806	21·1
13	w	0.879	21·2

Simultaneous solution of these two equations gives $a = 2.66$ Å, $c = 4.94$ Å, and $c/a = 1.86$.

Rhombohedral System

Rhombohedral crystals are also characterized by unit cells having two parameters, in this case a and α. No new chart is needed, however, to index the patterns of rhombohedral substances, because, as mentioned in Sec. 2–4, any rhombohedral crystal may be referred to hexagonal axes. A hexagonal Hull–Davey or Bunn chart may therefore be used to index the pattern of a rhombohedral crystal. The indices so found will, of course, refer to a hexagonal cell, and the method of converting them to rhombohedral indices is described in Appendix 4.

We can conclude that the pattern of any two-parameter crystal (tetragonal, hexagonal, or rhombohedral) can be indexed on the appropriate Hull–Davey or Bunn chart. If the structure is known, the procedure is quite straightforward. The best method is to calculate the c/a ratio from the known parameters, lay a straightedge on the chart to discover the proper line sequence for this value of c/a, calculate the value of $\sin^2\theta$ for each line from the indices found on the chart, and then determine the indices of the observed lines by a comparison of calculated and observed $\sin^2\theta$ values.

If the structure is unknown, the problem of indexing is not always so easy as it seems in theory. The most common source of trouble is the presence of extraneous lines, as defined in Sec. 10–2, in the observed pattern. Such lines can be very confusing and, if any difficulty in indexing is encountered, every effort should be made to eliminate them from the pattern, either experimentally or by calculation. In addition, the observed $\sin^2\theta$ values usually contain systematic errors which make a simultaneous fit of all the pencil marks on the paper strip to curves on the chart impossible, even when the paper strip is at the correct c/a position. Because of these errors, the strip has to be shifted slightly from line to line in order to make

successive pencil marks coincide with curves on the chart. Two important rules must always be kept in mind when using Hull–Davey or Bunn charts:

1. Every mark on the paper strip must coincide with a curve on the chart, except for extraneous lines. A structure which accounts for only a portion of the observed lines is not correct: *all* the lines in the pattern must be accounted for, either as due to the structure of the substance involved or as extraneous lines.

2. There need not be a mark on the paper strip for every curve on the chart, because some lines may have zero intensity or be too weak to be observed.

Orthorhombic, Monoclinic, and Triclinic Systems

Substances with these low-symmetry structures yield powder patterns which are almost impossible to index by graphical methods, although the patterns of some orthorhombic crystals have been indexed by a combination of graphical and analytical methods. The essential difficulty is the large number of variable parameters involved. In the orthorhombic system there are three such parameters (a, b, c), in the monoclinic four (a, b, c, β), and in the triclinic six (a, b, c, α, β, γ). If the structure is known, patterns of substances in these crystal systems can be indexed by comparison of the observed $\sin^2\theta$ values with those calculated for all possible values of hkl.

10–5 INDEXING PATTERNS OF NONCUBIC CRYSTALS (ANALYTICAL METHODS)

Analytical methods of indexing involve arithmetical manipulation of the observed $\sin^2\theta$ values in an attempt to find certain relationships among them. Since each crystal system is characterized by particular relationships between $\sin^2\theta$ values, recognition of these relationships identifies the crystal system and leads to a solution of the line indices. These analytical methods are due mainly to Hesse and Lipson [10.4, 10.5, G.8, G.32, G.17].

Tetragonal System

Here the $\sin^2\theta$ values must obey the relation:

$$\sin^2\theta = A(h^2 + k^2) + Cl^2, \tag{10–7}$$

where A $(= \lambda^2/4a^2)$ and C $(= \lambda^2/4c^2)$ are constants for any one pattern. The problem is to find these constants, since, once found, they will disclose the cell parameters a and c and enable the line indices to be calculated. The value of A is obtained from the $hk0$ lines. When $l = 0$, Eq. (10–7) becomes

$$\sin^2\theta = A(h^2 + k^2).$$

The permissible values of $(h^2 + k^2)$ are 1, 2, 4, 5, 8, etc. Therefore the $hk0$ lines must have $\sin^2\theta$ values in the ratio of these integers, and A will be some number which is 1, $\frac{1}{2}$, $\frac{1}{4}$, $\frac{1}{5}$, $\frac{1}{8}$, etc., times the $\sin^2\theta$ values of these lines. C is obtained from the other lines on the pattern and the use of Eq. (10–7) in the form

$$\sin^2\theta - A(h^2 + k^2) = Cl^2.$$

Differences represented by the left-hand side of the equation are set up, for various assumed values of h and k, in an attempt to find a consistent set of Cl^2 values, which must be in the ratio 1, 4, 9, 16, etc. Once these values are found, C can be calculated.

Hexagonal System

For hexagonal crystals, an exactly similar procedure is used. In this case, $\sin^2\theta$ values are given by

$$\sin^2\theta = A(h^2 + hk + k^2) + Cl^2,$$

where $A = \lambda^2/3a^2$ and $C = \lambda^2/4c^2$. Permissible values of $(h^2 + hk + k^2)$ are tabulated in Appendix 10; they are 1, 3, 4, 7, 9, etc. The indexing procedure is best illustrated by means of a specific example, namely, the powder pattern of zinc, whose observed $\sin^2\theta$ values are listed in Table 10–2. We first divide the $\sin^2\theta$ values by the integers 1, 3, 4, etc., and tabulate the results, as shown by Table 10–3, which applies to the first six lines of the pattern. We then examine these numbers, looking for quotients which are equal to one another or equal to one of the observed $\sin^2\theta$ values. In this case, the two starred entries, 0.112 and 0.111, are the most nearly equal, so we assume that lines 2 and 5 are $hk0$ lines. We then tentatively put $A = 0.112$ which is equivalent to saying that line 2 is 100. Since the $\sin^2\theta$ value of line 5 is very nearly 3 times that of line 2, line 5 should be 110. To find the value of C, we must use the equation

$$\sin^2\theta - A(h^2 + hk + k^2) = Cl^2.$$

We now subtract from each $\sin^2\theta$ value the values of A (= 0.112), $3A$ (= 0.336), $4A$ (= 0.448), etc., and look for remainders (Cl^2) which are in the ratio of 1, 4, 9, 16, etc. These figures are given in Table 10–4. Here the five starred entries are of interest, because these numbers (0.024, 0.097, 0.221, and 0.390) are very nearly in the ratio 1, 4, 9, and 16. We therefore put $0.024 = C(1)^2$, $0.097 = C(2)^2$, $0.221 = C(3)^2$, and $0.390 = C(4)^2$. This gives $C = 0.024$ and immediately identifies line 1 as 002 and line 6 as 004. Since line 3 has a $\sin^2\theta$ value equal to the sum of A and C, its indices must be 101. Similarly, the indices of lines 4 and 5 are found to be 102 and 103, respectively. In this way, indices are assigned to all the lines on the pattern, and a final check on their correctness is made in the usual manner, by a comparison of observed and calculated $\sin^2\theta$ values.

Table 10–3

Line	$\sin^2\theta$	$\frac{\sin^2\theta}{3}$	$\frac{\sin^2\theta}{4}$	$\frac{\sin^2\theta}{7}$	hkl
1	0.097	0.032	0.024	0.014	
2	0.112*	0.037	0.028	0.016	100
3	0.136	0.045	0.034	0.019	
4	0.209	0.070	0.052	0.030	
5	0.332	0.111*	0.083	0.047	110
6	0.390	0.130	0.098	0.056	

Table 10–4

Line	$\sin^2\theta$	$\sin^2\theta - A$	$\sin^2\theta - 3A$	hkl
1	0.097*			002
2	0.112	0.000*		100
3	0.136	0.024*		101
4	0.209	0.097*		102
5	0.332	0.221*		110, 103
6	0.390*	0.278	0.054	004

Orthorhombic System

The basic equation governing the $\sin^2\theta$ values is now

$$\sin^2\theta = Ah^2 + Bk^2 + Cl^2.$$

The indexing problem is considerably more difficult here, in that three unknown constants, A, B, and C, have to be determined. The general procedure, which is too lengthy to illustrate here, is to search for significant differences between various pairs of $\sin^2\theta$ values. For example, consider any two lines having indices $hk0$ and $hk1$, with hk the same for each, such as 120 and 121; the difference between their $\sin^2\theta$ values is C. Similarly, the difference between the $\sin^2\theta$ values of two lines such as 310 and 312 is $4C$, and so on. If the structure is such that there are many lines missing from the pattern, because of a zero structure factor for the corresponding planes, then the difficulties of indexing are considerably increased, inasmuch as the missing lines may be the very ones which would supply the most easily recognized clues if they were present. Despite such difficulties, this analytical method has been applied successfully to a number of orthorhombic patterns. One requisite for its success is fairly high accuracy in the $\sin^2\theta$ values (at least ± 0.0005), and the investigator should therefore correct his observations for systematic errors before attempting to index the pattern.

Monoclinic and Triclinic Systems

These crystal systems involve four and six independent constants, respectively. The corresponding powder patterns are of great complexity and may contain more than a hundred lines. Such patterns are seldom solved without the aid of the computer.

General

Analytical methods of indexing are search procedures designed to reveal certain numerical relationships among the observed $\sin^2\theta$ values. The digital computer is therefore a natural tool to use, and many computer programs have been written for the indexing of powder patterns. Klug and Alexander [G.39] have surveyed the general problems involved and give references to specific programs.

Computer indexing is not always successful. The computer may yield not one but many sets of indices that approximately conform to the input data; it is then up to the investigator's experience and judgment to select the correct set. Extra-

neous diffraction lines and inaccurate $\sin^2 \theta$ values can mislead a computer as well as a human searcher.

The powder patterns of low-symmetry substances are so difficult to solve that the crystal structures of such substances are almost always determined by examining a single crystal, by either the rotating-crystal method or one of its variations. With these methods the x-ray crystallographer can, without much difficulty, determine the shape and size of an unknown unit cell, no matter how low its symmetry. Many substances are very difficult to prepare in single-crystal form, but, on the other hand, if the substance involved is one of low symmetry, the time spent in trying to obtain a single crystal is usually more fruitful than the time spent in trying to solve the powder pattern. The single-crystal specimen need not be large: a crystal as small as 0.1 mm in any dimension can be successfully handled and will give a satisfactory diffraction pattern.

10–6 THE EFFECT OF CELL DISTORTION ON THE POWDER PATTERN

At this point we might digress slightly from the main subject of this chapter, and examine some of the changes produced in a powder pattern when the unit cell of the substance involved is distorted in various ways. As we have already seen, there are many more lines on the pattern of a substance of low symmetry, such as triclinic, than on the pattern of a substance of high symmetry, such as cubic, and we may take it as a general rule that any distortion of the unit cell which decreases its symmetry, in the sense of introducing additional variable parameters, will increase the number of lines on the powder pattern.

Figure 10–5 graphically illustrates this point. On the left is the calculated diffraction pattern of the body-centered cubic substance whose unit cell is shown at the top. The line positions are computed for $a = 4.00$ Å and Cr $K\alpha$ radiation. If this cell is expanded or contracted uniformly but still remains cubic, the diffraction lines merely shift their positions but do not increase in number, since no change in cell symmetry is involved. However, if the cubic cell is distorted along only one axis, then it becomes tetragonal, its symmetry decreases, and more diffraction lines are formed. The center pattern shows the effect of stretching the cubic cell by 4 percent along its [001] axis, so that c is now 4.16 Å. Some lines are unchanged in position, some are shifted, and new lines have appeared. If the tetragonal cell is now stretched by 8 percent along its [010] axis, it becomes orthorhombic, with $a = 4.00$ Å, $b = 4.32$ Å, and $c = 4.16$ Å, as shown on the right. The result of this last distortion is to add still more lines to the pattern. The increase in the number of lines is due essentially to the introduction of new plane spacings, caused by nonuniform distortion. Thus, in the cubic cell, the (200), (020), and (002) planes all have the same spacing and only one line is formed, called the 200 line, but this line splits into two when the cell becomes tetragonal, since now the (002) plane spacing differs from the other two. When the cell becomes orthorhombic, all three spacings are different and three lines are formed.

Changes of this nature are not uncommon among phase transformations and ordering reactions. For example, the powder pattern of slowly cooled plain carbon steel shows lines due to ferrite (body-centered cubic) and cementite (Fe_3C,

Fig.
con

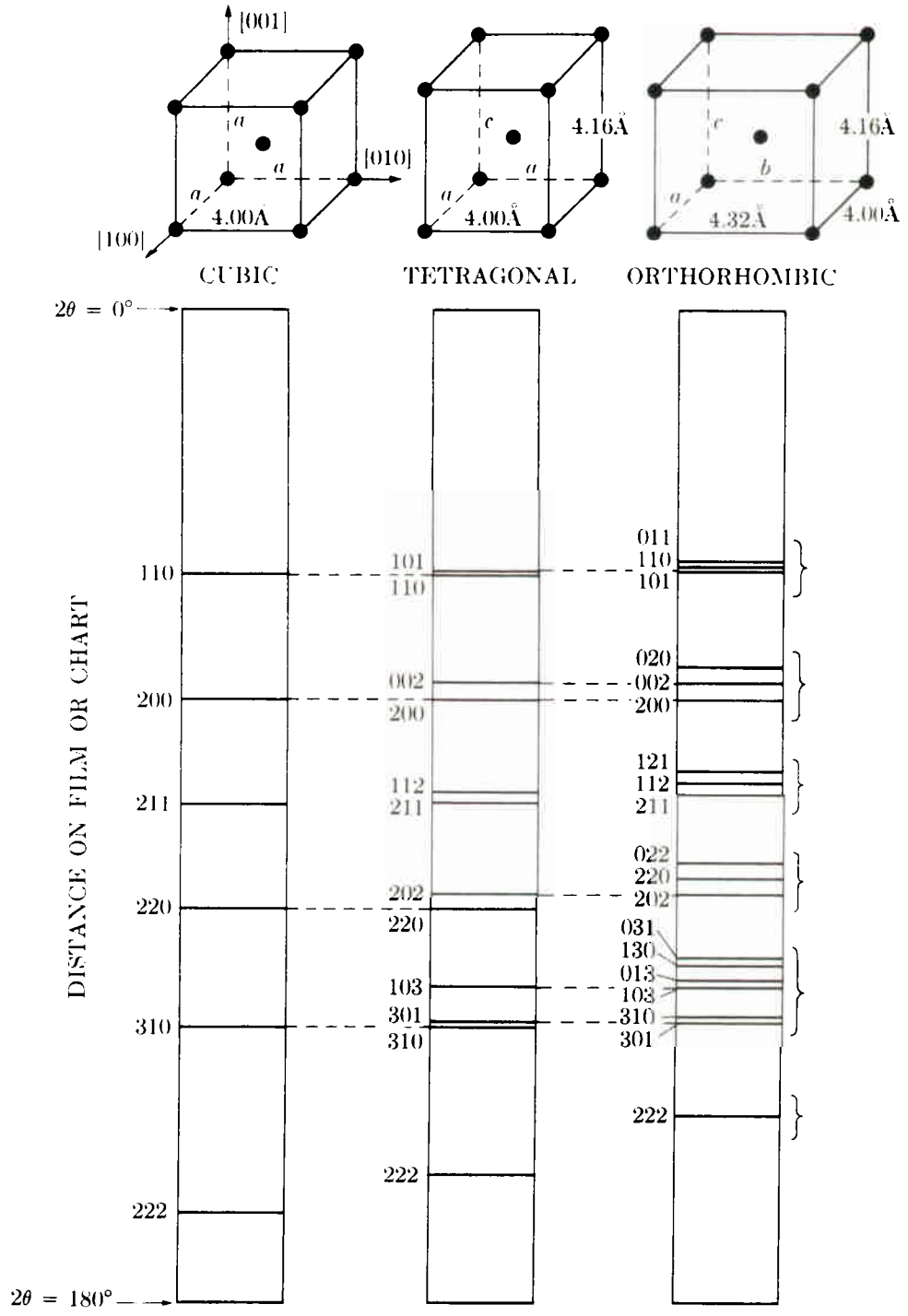

Fig. 10–5 Effects of cell distortion on powder patterns. Lines unchanged in position are connected by dashed lines.

orthorhombic). When the same steel is quenched from the austenite region, the phases present are martensite (body-centered tetragonal) and, possibly, some untransformed austenite (face-centered cubic). The a and c parameters of the martensite cell do not differ greatly from the a parameter of the ferrite cell (see Fig. 12–5). The result is that the diffraction pattern of a quenched steel shows pairs of martensite lines occurring at about the same 2θ positions as the individual lines of ferrite in the previous pattern. (These line pairs, however, are seldom resolved; martensite contains so much microstrain that each line of a pair is so broad that it merges with its neighbor.) If the quenched steel is now tempered, the martensite will ultimately decompose into ferrite and cementite, and each pair of martensite lines will coalesce into a single ferrite line. Somewhat similar effects can be produced in a copper-gold alloy having the composition represented by the formula AuCu. This alloy is cubic in the disordered state but becomes either tetragonal or orthorhombic when ordered, depending on the ordering temperature (see Sec. 13–3).

The changes produced in a powder pattern by cell distortion depend, in degree, on the amount of distortion. If the latter is small, the pattern retains the main features of the pattern of the original undistorted cell. Thus, in Fig. 10–5, the nineteen lines of the orthorhombic pattern fall into the six bracketed groups shown, each group corresponding to one of the single lines on the cubic pattern. In fact, an experienced crystallographer, if confronted with this orthorhombic pattern, might recognize this grouping and guess that the unit cell of the substance involved was not far from cubic in shape, and that the Bravais lattice was either simple or body-centered, since the groups of lines are spaced in a fairly regular manner. But if the distortion of the cubic cell had been much larger, each line of the original pattern would split into such widely separated lines that no features of the original pattern would remain.

10–7 DETERMINATION OF THE NUMBER OF ATOMS IN A UNIT CELL

To return to the subject of structure determination, the next step after establishing the shape and size of the unit cell is to find the number of atoms in that cell, because the number of atoms must be known before their positions can be determined. To find this number we use the fact that the volume of the unit cell, calculated from the lattice parameters by means of the equations given in Appendix 3, multiplied by the measured density of the substance equals the weight of all the atoms in the cell. From Eq. (3–7), we have

$$\sum A = \frac{\rho V'}{1.66042},$$

where $\sum A$ is the sum of the atomic weights of the atoms in the unit cell, ρ is the density (gm/cm^3), and V' is the volume of the unit cell (Å^3). If the substance is an element of atomic weight A, then

$$\sum A = n_1 A,$$

where n_1 is the number of atoms per unit cell. If the substance is a chemical compound, or an intermediate phase whose composition can be represented by a

simple chemical formula, then

$$\sum A = n_2 M,$$

where n_2 is the number of "molecules" per unit cell and M the molecular weight. The number of atoms per cell can then be calculated from n_2 and the composition of the phase.

When determined in this way, the number of atoms per cell is always an integer, within experimental error, except for a very few substances which have "defect structures." In these substances, atoms are simply missing from a certain fraction of those lattice sites which they would be expected to occupy, and the result is a nonintegral number of atoms per cell. FeO and the β phase in the Ni-Al system are examples.

10–8 DETERMINATION OF ATOM POSITIONS

We now have to find the positions of a known number of atoms in a unit cell of known shape and size. To solve this problem, we must make use of the observed relative *intensities* of the diffracted beams, since these intensities are determined by atom positions. In finding the atom positions, however, we must again proceed by trial and error, because there is no known general method of directly calculating atom positions from observed intensities.

To see why this is so, we must consider the two basic equations involved, namely,

$$I = |F|^2 p \left(\frac{1 + \cos^2 2\theta}{\sin^2 \theta \cos \theta} \right), \tag{4–19}$$

which gives the relative intensities of the reflected beams, and

$$F = \sum_1^N f_n e^{2\pi i(hu_n + kv_n + lw_n)}, \tag{4–11}$$

which gives the value of the structure factor F for the hkl reflection in terms of the atom positions uvw. Since the relative intensity I, the multiplicity factor p, and the Bragg angle θ are known for each line on the pattern, we can find the value of $|F|$ for each reflection from Eq. (4–19). But $|F|$ measures only the relative amplitude of each reflection, whereas, in order to use Eq. (4–11) for calculating atom positions, we must know the value of F, which measures both the amplitude *and* phase of one reflection relative to another. This is the crux of the problem. The intensities of two reflected beams are proportional to the squares of their amplitudes but independent of their relative phase. Since all we can measure is intensity, we can determine amplitude but not phase, which means that we cannot, in general, compute the structure factor but only its absolute value. This "phase problem," which had baffled crystallographers for years, has now been partially solved, in the sense that direct methods of structure determination, applicable to some structures, now exist. These methods have a success rate of 80 to 90 percent when applied to crystals with a hundred atoms or less per unit cell. Protein crystals, however, contain thousands of atoms per cell. No direct method has yet been found powerful enough to solve the structure of *any* crystal.

Atom positions, therefore, can be determined only by trial and error. A set of atom positions is assumed, the intensities corresponding to these positions are calculated, and the calculated intensities are compared with the observed ones, the process being repeated until satisfactory agreement is reached. The problem of selecting a structure for trial is not as hopelessly broad as it sounds, since the investigator has many aids to guide him. Foremost among these is the accumulated knowledge of previously solved structures. From these known structures he may be able to select a few likely candidates, and then proceed on the assumption that his unknown structure is the same as, or very similar to, one of these known ones. A great many known structures may be classified into groups according to the kind of bonding (ionic, covalent, metallic, or mixtures of these) which holds the atoms together, and a selection among these groups is aided by a knowledge of the probable kind of atomic bonding in the unknown phase, as judged from the positions of its constituent elements in the periodic table. For example, suppose the phase of unknown structure has the chemical formula AB, where A is strongly electropositive and B strongly electronegative, and that its powder pattern is characteristic of a simple cubic lattice. Then the bonding is likely to be ionic, and the CsCl structure is strongly suggested. But the FeSi structure shown in Fig. 2–20 is also a possibility. In this particular case, one or the other can be excluded by a density measurement, since the CsCl cell contains one "molecule" and the FeSi cell four. If this were not possible, diffracted intensities would have to be calculated on the basis of each cell and compared with the observed ones. It is this simple kind of structure determination, illustrated by an example in the next section, that the metallurgist should be able to carry out unaided.

Needless to say, many structures are too complex to be solved by this simple approach and the crystallographer must turn to more powerful methods. Chief among these are space-group theory and Fourier series. Although any complete description of these subjects is beyond the scope of this book, a few general remarks may serve to show their utility in structure determination. The *theory of space groups*, one of the triumphs of mathematical crystallography, relates crystal symmetry, on the atomic scale, to the possible atomic arrangements which possess that symmetry. For example, if a given substance is known to be hexagonal and to have n atoms in its unit cell, then space-group theory lists all possible arrangements of n atoms which will have hexagonal symmetry. This listing of possible arrangements aids tremendously in the selection of trial structures. A further reduction in the number of possibilities can then be made by noting the indices of the reflections absent from the diffraction pattern. By such means alone, i.e., before any detailed consideration is given to relative diffracted intensities, space-group theory can often exclude all but two or three possible atomic arrangements. There are 230 different space groups, and the possible atomic arrangements in each group are listed in [G.11, Vol. 1].

A *Fourier series* is a type of infinite trigonometric series by which any kind of periodic function may be expressed. Now the one essential property of a crystal is that its atoms are arranged in space in a periodic fashion. But this means that the density of electrons is also a periodic function of position in the crystal, rising

to a maximum at the point where an atom is located and dropping to a low value in the region between atoms. To regard a crystal in this manner, as a positional variation of electron density rather than as an arrangement of atoms, is particularly appropriate where diffraction is involved, in that x-rays are scattered by electrons and not by atoms as such. Since the electron density is a periodic function of position, a crystal may be described analytically by means of Fourier series. This method of description is very useful in structure determination because it can be shown that the coefficients of the various terms in the series are related to the F values of the various x-ray reflections. But such a series is not of immediate use, since the structure factors are not usually known both in magnitude and phase. However, another kind of series has been devised, called the Patterson function, whose coefficients are related to the experimentally observable $|F|$ values and which gives, not electron density, but information regarding the various interatomic vectors in the unit cell. This information is frequently enough to determine the phase of the various structure factors; then the first kind of series can be used to map out the actual electron density throughout the cell and thus disclose the atom positions.

10–9 EXAMPLE OF STRUCTURE DETERMINATION

As a simple example, we will consider an intermediate phase which occurs in the cadmium-tellurium system. Chemical analysis of the specimen, which appeared essentially one phase under the microscope, showed it to contain 46.6 weight percent Cd and 53.4 weight percent Te. This is equivalent to 49.8 atomic percent Cd and can be represented by the formula CdTe. The specimen was reduced to powder and a diffraction pattern obtained with a Debye–Scherrer camera and Cu $K\alpha$ radiation.

The observed values of $\sin^2\theta$ for the first 16 lines are listed in Table 10–5, together with the visually estimated relative line intensities. This pattern can be indexed on the basis of a cubic unit cell, and the indices of the observed lines are given in the table. The lattice parameter, calculated from the $\sin^2\theta$ value for the highest-angle line, is 6.46 Å.

The density of the specimen, as determined by weighing a quantity of the powder in a pyknometer bottle, was 5.82 gm/cm^3. We then find, from Eq. (3–7), that

$$\sum A = \frac{(5.82)(6.46)^3}{1.66042} = 945.$$

Since the molecular weight of CdTe is 240.02, the number of "molecules" per unit cell is 945/240.02 = 3.94, or 4, within experimental error.

At this point, we know that the unit cell of CdTe is cubic and that it contains 4 "molecules" of CdTe, i.e., 4 atoms of cadmium and 4 atoms of tellurium. We must now consider possible arrangements of these atoms in the unit cell. First we examine the indices listed in Table 10–5 for evidence of the Bravais lattice. Since the indices of the observed lines are all unmixed, the Bravais lattice must be face-centered. (Not all possible sets of unmixed indices are present, however: 200, 420,

Table 10–5

Line	Intensity	$\sin^2\theta$	*hkl*
1	s	0.0462	111
2	vs	0.1198	220
3	vs	0.1615	311
4	vw	0.1790	222
5	m	0.234	400
6	m	0.275	331
7	s	0.346	422
8	m	0.391	511, 333
9	w	0.461	440
10	m	0.504	531
11	m	0.575	620
12	w	0.616	533
13	w	0.688	444
14	m	0.729	711, 551
15	vs	0.799	642
16	s	0.840	731, 553

600, 442, 622, and 640 are missing from the pattern. But these reflections may be too weak to be observed, and the fact that they are missing does not invalidate our conclusion that the lattice is face-centered.) Now there are two common face-centered cubic structures of the AB type, i.e., containing two different atoms in equal proportions, and both contain four "molecules" per unit cell: these are the NaCl structure [Fig. 2–18(b)] and the zinc-blende form of ZnS [Fig. 2–19(b)]. Both of these are logical possibilities even though the bonding in NaCl is ionic and in ZnS covalent, since both kinds of bonding have been observed in telluride structures.

The next step is to calculate relative diffracted intensities for each structure and compare them with experiment, in order to determine whether or not one of these structures is the correct one. If CdTe has the NaCl structure, then its structure factor for unmixed indices [see Example (e) of Sec. 4–6] is given by

$$\begin{aligned} F^2 &= 16(f_{Cd} + f_{Te})^2, \quad \text{if } (h + k + l) \text{ is even,} \\ F^2 &= 16(f_{Cd} - f_{Te})^2, \quad \text{if } (h + k + l) \text{ is odd.} \end{aligned} \tag{10–8}$$

On the other hand, if the ZnS structure is correct, then the structure factor for unmixed indices (see Sec. 4–13) is given by

$$\begin{aligned} |F|^2 &= 16(f_{Cd}^2 + f_{Te}^2), \quad \text{if } (h + k + l) \text{ is odd,} \\ |F|^2 &= 16(f_{Cd} - f_{Te})^2, \quad \text{if } (h + k + l) \text{ is an odd multiple of 2,} \\ |F|^2 &= 16(f_{Cd} + f_{Te})^2, \quad \text{if } (h + k + l) \text{ is an even multiple of 2.} \end{aligned} \tag{10–9}$$

Even before making a detailed calculation of relative diffracted intensities by means of Eq. (4–19), we can almost rule out the NaCl structure as a possibility simply by inspection of Eqs. (10–8). The atomic numbers of cadmium and tel-

lurium are 48 and 52, respectively, so the value of $(f_{Cd} + f_{Te})^2$ is several hundred times greater than the value of $(f_{Cd} - f_{Te})^2$, for all values of $\sin \theta/\lambda$. Then, if CdTe has the NaCl structure, the 111 reflection should be very weak and the 200 reflection very strong. Actually, 111 is strong and 200 is not observed. Further evidence that the NaCl structure is incorrect is given in the fourth column of Table 10–6, where the calculated intensities of the first eight possible lines are listed: there is no agreement whatever between these values and the observed intensities.

On the other hand, if the ZnS structure is assumed, intensity calculations lead to the values listed in the fifth column. The agreement between these values and the observed intensities is excellent, except for a few minor inconsistencies among the low-angle reflections, and these are due to neglect of the absorption factor. In particular, we note that the ZnS structure satisfactorily accounts for all the missing reflections (200, 420, etc.), since the calculated intensities of these reflections are all extremely low. We can therefore conclude that CdTe has the structure of the zinc-blende form of ZnS.

Table 10–6

1	2	3	4	5
Line	*hkl*	Observed intensity	Calculated intensity	
			NaCl structure	ZnS structure
1	111	s	0.05	12.4
	200	nil	13.2	0.03
2	220	vs	10.0 ← →	10.0
3	311	vs	0.02	6.2
4	222	vw	3.5	0.007
5	400	m	1.7	1.7
6	331	m	0.01	2.5
	420	nil	4.6	0.01
7	422	s	. . . . .	3.4
8	511, 333	m	. . . . .	1.8
9	440	w	. . . . .	1.1
10	531	m	. . . . .	2.0
	600, 442	nil	. . . . .	0.005
11	620	m	. . . . .	1.8
12	533	w	. . . . .	0.9
	622	nil	. . . . .	0.004
13	444	w	. . . . .	0.6
14	711, 551	m	. . . . .	1.8
	640	nil	. . . . .	0.005
15	642	vs	. . . . .	4.0
16	731, 553	s	. . . . .	3.3

(N.B. Calculated intensities have been adjusted so that the 220 line has an intensity of 10.0 for both structures.)

After a given structure has been shown to be in accord with the diffraction data, it is advisable to calculate the interatomic distances involved in that structure. This calculation not only is of interest in itself, but serves to disclose any gross errors that may have been made, since there is obviously something wrong with a proposed structure if it brings certain atoms impossibly close together. In the present structure, the nearest neighbor to the Cd atom at 0 0 0 is the Te atom at $\frac{1}{4}\,\frac{1}{4}\,\frac{1}{4}$. The Cd-Te interatomic distance is therefore $\sqrt{3}\,a/4 = 2.80$ Å. For comparison, we can calculate a "theoretical" Cd-Te interatomic distance simply by averaging the distances of closest approach in the pure elements. In doing this, we regard the atoms as rigid spheres in contact, and ignore the effects of coordination number and type of bonding on atom size. These distances of closest approach are 2.98 Å in pure cadmium and 2.86 Å in pure tellurium, the average being 2.92 Å. The observed Cd-Te interatomic distance is 2.80 Å, or some 4.1 percent smaller than the calculated value; this difference is not unreasonable and can be largely ascribed to the covalent bonding which characterizes this structure. In fact, it is a general rule that the A-B interatomic distance in an intermediate phase A_xB_y is always somewhat smaller than the average distance of closest approach in pure A and pure B, because the mere existence of the phase shows that the attractive forces between unlike atoms is greater than that between like atoms. If this were not true, the phase would not form.

PROBLEMS

***10–1** The powder pattern of aluminum, made with Cu $K\alpha$ radiation, contains ten lines, whose $\sin^2\theta$ values are 0.1118, 0.1487, 0.294, 0.403, 0.439, 0.583, 0.691, 0.727, 0.872, and 0.981. Index these lines and calculate the lattice parameter.

10–2 A pattern is made of a cubic substance with unfiltered chromium radiation. The observed $\sin^2\theta$ values and intensities are 0.265(m), 0.321(vs), 0.528(w), 0.638(s), 0.793(s), and 0.958(vs). Index these lines and state which are due to $K\alpha$ and which to $K\beta$ radiation. Determine the Bravais lattice and lattice parameter. Identify the substance by reference to Appendix 5.

10–3 Construct a Hull–Davey chart, and accompanying $\sin^2\theta$ scale, for hexagonal close-packed lattices. Use two-range semilog graph paper, $8\frac{1}{2} \times 11$ in. Cover a c/a range of 0.5 to 2.0, and plot only the curves $00 \cdot 2$, $10 \cdot 0$, $10 \cdot 1$, $10 \cdot 2$, and $11 \cdot 0$.

***10–4** Use the chart constructed in Prob. 10–3 to index the first five lines on the powder pattern of α-titanium. With Cu $K\alpha$ radiation, these lines have the following $\sin^2\theta$ values: 0.091, 0.106, 0.117, 0.200, and 0.268.

In each of the following problems the powder pattern of an element is represented by the observed $\sin^2\theta$ *values of the first seven or eight lines on the pattern, made with Cu* $K\alpha$ *radiation. In each case, index the lines, find the crystal system, Bravais lattice, and approx-*